Chemistry–A European Journal
Research Article
doi.org/10.1002/chem.202303783
Chemistry Europe
European Chemical Societies Publishing
www.chemeurj.org

# Redox-Mediated Amination of Pyrogallol-Based Polyphenols

Salavat S. Ashirbaev,[a] Natércia F. Brás,*[a, b] Patricia Frei,[c] Kuangjie Liu,[a] Simone Moser,[d] and Hendrik Zipse*[a]

Flavonoids are known to covalently modify amyloidogenic peptides by amination reactions. The underlying coupling process between polyphenols and *N*-nucleophiles is assessed by several *in vitro* and *in silico* approaches. The coupling reaction involves a sequence of oxidative dearomatization, amination, and reductive amination (ODARA) reaction steps. The C6-regioselectivity of the product is confirmed by crystallographic analysis. Under aqueous conditions, the reaction of baicalein with lysine derivatives yields C–N coupling as well as hydrolysis products of transient imine intermediates. The observed C–N coupling reactions work best for flavonoids combining a pyrogallol substructure with an electron-withdrawing group attached to the C4a-position. Thermodynamic properties such as bond dissociation energies also highlight the key role of pyrogallol units for the antioxidant ability. Combining the computed electronic properties and *in vitro* antioxidant assays suggests that the studied pyrogallol-containing flavonoids act by various radical-scavenging mechanisms working in synergy. Multivariate analysis indicates that a small number of descriptors for transient intermediates of the ODARA process generates a model with excellent performance ($r = 0.93$) for the prediction of cross-coupling yields. The same model has been employed to predict novel antioxidant flavonoid-based molecules as potential covalent inhibitors, opening a new avenue to the design of therapeutically relevant anti-amyloid compounds.

## Introduction

Polyphenols, a broad class of antioxidants found in fruits, vegetables, and other sources, are sensitive to oxidation. As a result, they can be easily converted into their oxidized quinone forms, which have the potential to interact with neighboring functional groups. In general, quinones are used as redox cofactors in various enzymatic processes, examples being topaquinone (TPQ) and pyrroloquinoline quinone (PQQ) found in enzymes catalyzing the oxidation of amines and alcohols.[1] Significant effort has been made to mimic their reactivity with synthetic quinones in catalytic processes.[2] The reaction of polyphenols with amines as well as ammonia is known to proceed readily under aerobic conditions.[3] While C–N coupling products appear to be formed in all of these reactions, the regiochemistry of product formation is often not clarified.[4] Mechanistic studies on the catalytic potential of pyrogallol-based polyphenols by Largeron *et al.* highlight the importance of transient *ortho*-quinones and their respective imine derivatives.[5] *In vivo* formation of $NH_2$-metabolites of flavonoids such as baicalein (BA, **1a**), myricetin, and (−)-epigallocatechin (EGC) have been reported.[6] Similarly, the formation of a covalent adduct of **1a** with human islet amyloid polypeptide (hIAPP, amylin) has been demonstrated (Scheme 1a).[7]

The solution phase reaction of baicalein (**1a**) with pentylamine (**2a**) has recently been described in the context of a model study for the reaction of polyphenol antioxidants with hIAPP (Scheme 1b). Pentylamine (**2a**) was chosen to model the *N*-terminal Lys residue of hIAPP on the basis of closely similar $pK_a$ characteristics and steric demand.[8] Covalent adduct formation of polyphenols with amyloidogenic proteins through lysine-derived cross-links are particularly relevant in the context of redirecting the components of insoluble aggregates back to soluble monomers. Indeed, earlier studies showed that oxidized forms of flavonoids such as **1a** and epigallocatechin gallate (EGCG) inhibit fibrillation of amyloidogenic peptides and/or disaggregate fibrils.[9] The peptide adducts may exhibit different cytotoxicity or biological functions, while the polyphenol's antioxidant properties usually increase.[10] One of the main goals of this work is to explore the possible amination reaction of **1a**

[a] S. S. Ashirbaev, Dr. N. F. Brás, K. Liu, Prof. Dr. H. Zipse
Department of Chemistry
Ludwig Maximilian University of Munich
Butenandtstraße 5–13, 81377, Munich, Germany
E-mail: zipse@cup.uni-muenchen.de
natercia.braz@cup.uni-muenchen.de
[b] Dr. N. F. Brás
LAQV, REQUIMTE, Departamento de Química e Bioquímica, Faculdade de Ciências
Universidade do Porto
Rua do Campo Alegre s/n, 4169-007 Porto, Portugal
E-mail: nbras@fc.up.pt
[c] P. Frei
Department of Pharmacy
Ludwig Maximilian University of Munich
Butenandtstraße 5–13, 81377, Munich, Germany
[d] Prof. Dr. S. Moser
Institute of Pharmacy
University of Innsbruck
Innrain 80–13, 6020, Innsbruck, Austria

Supporting information for this article is available on the WWW under https://doi.org/10.1002/chem.202303783

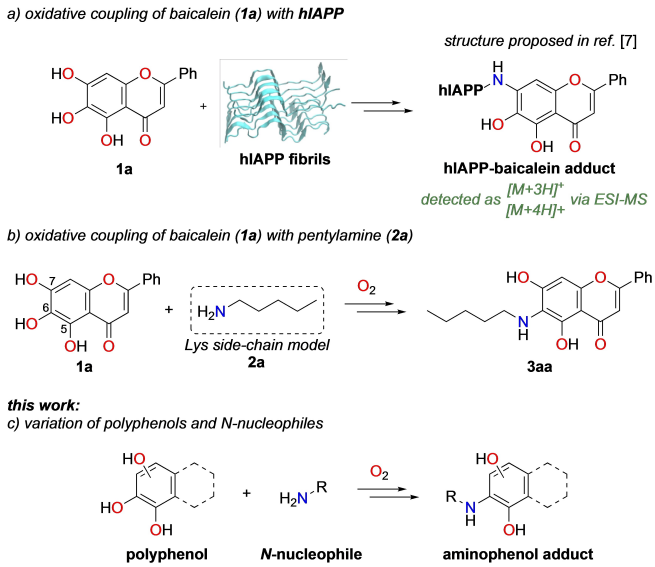


**Scheme 1.** Oxidative coupling of phenols with *N*-nucleophiles.

and other antioxidants based on the pyrogallol subunit with primary amines and peptide models (Scheme 1c). Furthermore, defining the redox properties of flavonoids and their amine conjugates is relevant for understanding redox-based therapeutic responses. Thermodynamic properties such as the bond dissociation energy (BDE), ionization potential (IP), proton affinity (PA), and electron transfer enthalpies (ETEs) provide a quantitative basis for the assessment of radical-scavenging activities of flavonoids.[11] *In vitro* assays such as FRAP (ferric reducing antioxidant power) and ORAC (oxygen radical absorbance capacity) have also been used widely for the same purpose.[11a] For a library of 25 polyphenols we therefore report theoretically calculated redox energetics as well as the results of FRAP and ORAC assays. The combination of *in silico* and *in vitro* data points to the main antioxidant mechanisms involved.

## Results and Discussion

### Mechanistic Studies

Baicalein (**1a**), insoluble in DCM, reacts with pentylamine (**2a**), giving 11% and 72% yield of **3aa** in 1 h and 18 h, correspondingly, under $O_2$ atmosphere at 23 °C (Scheme 2). The isolated product **3aa** shows that the C6-OH substituent of **1a** is replaced by a pentylamine fragment in an overall redox-neutral (but redox-mediated and thus oxygen-dependent) reaction mechanism. The C6-regioselectivity of the reaction is confirmed by sc-XRD analysis of the obtained crystals of **3aa** (Figure 1).

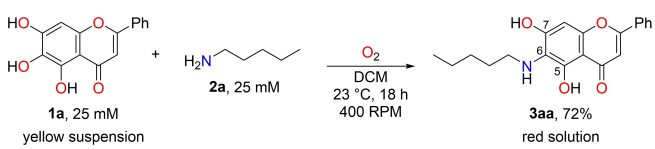


**Scheme 2.** Oxidative coupling of **1a** and **2a**.

Closer analysis of the obtained X-ray structure shows that the unit cell consists of two molecules of **3aa**, one in a zwitterionic and one in an internally neutral form, connected by a low-barrier hydrogen bond (O5–H···O1). This kind of bonding can occur when two tautomeric forms have closely similar stabilities,[12] which is supported by DFT calculations at SMD(water)/B3LYP-D3/6-31+G(d,p) level indicating a stability difference of 0.3 kJ/mol (see section SI-B 6).

To assess the propensity of other substrates to undergo the amination reaction observed for **1a**, it is helpful to analyse the requirements of all stages of the proposed reaction mechanism. For detailed mechanistic studies we therefore selected 2,3,4-trihydroxyacetophenone (TAP, **1b**) as a functional and structural model for baicalein (**1a**). The reaction of **1b** with **2a** has been analysed in different reaction media and under various reaction conditions to further elucidate the nature of this reaction and its role in the inhibition of hIAPP aggregation.

As depicted in Scheme 3, the formation of covalent adduct **3ba** proceeds through an *ortho*-quinone chain mechanism A (Scheme 3, green area). Initiation of this process involves acid/base reaction of **1b** with **2a** such that a phenolate/ammonium ion pair **1b-2a** of low solubility is formed, whose structure was confirmed via sc-XRD analysis.[8] Oxidative coupling of **1b** with a 3-fold excess of **2a** proceeds only slowly under air in DCM (4% yield, Table 1, Entry 1). Replacing air with a pure oxygen atmosphere leads to moderately increased conversion (27% yield of **3ba**, Table 1, Entry 2). The low reactivity is rationalized by the low solubility of the reacting ion pair **1b**–**2a** in DCM. To demonstrate this, the reaction medium is spiked with 10 vol% [D6]DMSO, which significantly increases the rate of the oxidative coupling and gives 88% of **3ba** (Table 1, Entry 16). Once the phenolate ion pair **1b**–**2a** is dissolved, it reacts with oxygen through single electron transfer (SET) to yield superoxide and a phenoxy radical complex, followed by a hydrogen atom transfer (HAT) step to yield perhydroxyl anion $HO_2^-$ and *ortho*-quinone **4b**. We note in passing that the stability of the

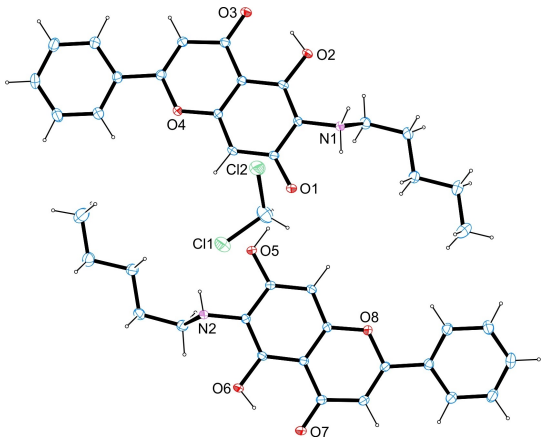


**Figure 1.** Crystal structure of coupling product **3aa** crystallized from DCM (ellipsoids shown at 25% probability level).

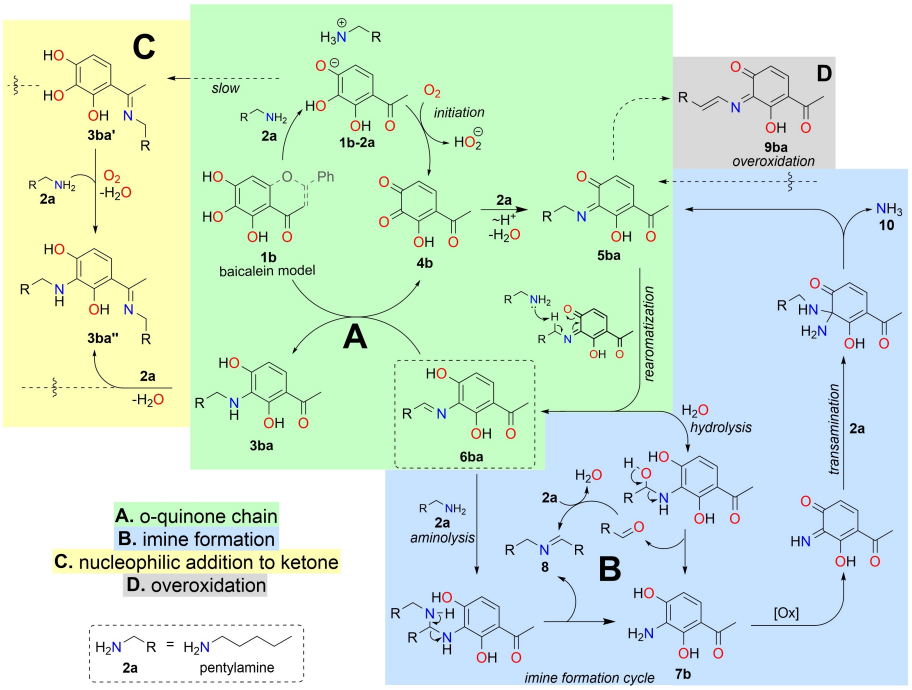


**Scheme 3.** Proposed mechanism of **1b**–**2a** oxidative coupling. All numbered structures were detected *via* NMR or APCI-MS.

transient phenoxy radical is directly related to the O–H bond dissociation energy (BDE) in polyphenol as indicated by the dotted arrow in Scheme 4. Formed **4b** is expected to react rapidly with **2a** to the respective imine **5ba**, followed by intramolecular or intermolecular isomerization to α-imine **6ba** and the transfer-hydrogenation step with **1b** to complete the formation of amination product **3ba**. The overall process can be characterized as an oxidative dearomatization, amination and reductive aromatization (ODARA) process.

Pentylamine (**2a**) most likely acts as a proton transfer catalyst in the rearomatization step, because the overall rate of the reaction is found to increase up to 2 eq of **2a** (80% yield) (Table 1, Entries 3–16). Similarly high yields can be obtained by combining 1 eq of **2a** with a sterically hindered catalytic base such as 1 eq of *t*-BuNH$_2$ (75% yield) or 0.1 eq of DBU (70% yield) as shown in Table 1 in entries 8 and 9. Quantum chemical calculations at the DLPNO-CCSD(T)/CBS//SMD(water)/B3LYP-D3/6-31+G(d,p) level of theory predict that the activation energy for the isomerization of **5ba** to **6ba** drops from +90.2 kJ/mol in the absence of a protic catalyst to +56.6 kJ/mol in the presence of **2a** as the catalyst. In both cases the isomerization reaction is highly exothermic at −111.9 kJ/mol (see section SI-B1). Closer analysis of the obtained reaction mixtures by $^1$H NMR spectroscopy indicates that the addition of [D6]DMSO is accompanied by the formation of minor product **7b** and a comparable amount of dipentylimine (DPI, **8**). With reference to the reaction network shown in Scheme 3, this result can be understood as an increased population of the area described as the imine formation region **B** (blue area). The key intermediate linking area **A** and **B** is transient imine **6ba**, whose addition reaction with a second equivalent pentylamine leads to dipentylimine (**8**) and aminophenol **7b** in a stepwise manner. Alternatively, imine **8** can also be formed through hydrolysis of **6ba** to aminophenol **7b** and pentanal, and subsequent condensation of this latter compound with one equivalent of amine **2a**. Both pathways involve formation of aminophenol **7b**, whose oxidation and transamination with pentylamine (**2a**) feeds back into the reaction network at the stage of imine **5ba**. Perusal of the product distribution data in Table 1 shows that the formation of dipentylimine (**8**) is closely linked to solvent polarity. Practically no dipentylimine (and very little aminophenol **7b**) is formed in DCM as the solvent, while formation of both compounds becomes quite notable in DCM/10 vol% DMSO mixtures. Comparing entries 3 and 16 in Table 1, we also note that the ratio of product phenols **3ba**/**7b** depends inversely on the concentration of pentylamine (**2a**), reaching up to 88/11 when using 3.0 eq of **2a** (relative to reactant phenol **1b**). The reaction in neat [D6]DMSO then leads to formation of **7b** and **8** as the major products in 32% and 48% yield, correspondingly, and only a minor amount of **3ba** (6%). It should be added that reaction products **3ba** and **7b** can interconvert under selected reaction conditions. As illustrated in Scheme 5, reaction of **3ba** with pentylamine (**2a**) in [D6]DMSO gives equimolar amounts of **7b** (8.5%) and **8** (16%). Under the same conditions, the reaction

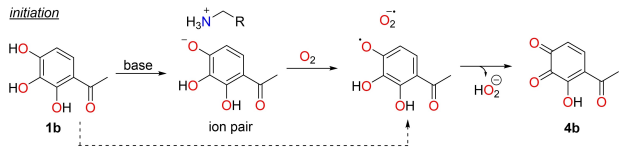


**Scheme 4.** Step-by-step oxidation of pyrogallol-based polyphenol.

**Table 1.** Oxidative coupling of **1b** with **2a**.

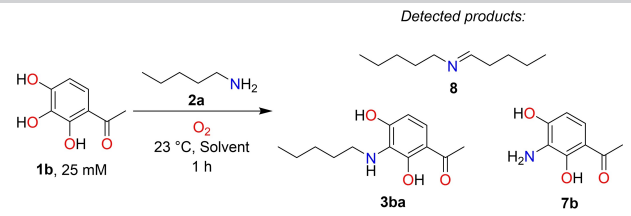


| # | Solvent | 2a, eq | Yield, %[a] | | |
|---|---|---|---|---|---|
| | | | 3ba | 7b | 8 |
| 1[b] | DCM | 3.00 | 4 | 2 | ND |
| 2 | | 3.00 | 27 | 2 | ND |
| 3 | [D2]DCM[c] | 0.20 | 6 | 3 | 7 |
| 4 | | 0.50 | 27 | 7 | 15 |
| 5 | | 1.00 | 42 | 7 | 13 |
| 6[d] | | | 45 | 8 | 15 |
| 7[e] | | | 30 | 11 | 20 |
| 8[f] | | | 75 | 11 | – |
| 9[g] | | | 70 | 14 | – |
| 10[h] | | | 34 | ND | 4 |
| 11 | | 1.15 | 52 | 8 | 14 |
| 12 | | 1.33 | 56 | 8 | 12 |
| 13 | | 1.75 | 75 | 10 | 11 |
| 14 | | 2.00 | 80 | 10 | 10 |
| 15[b] | | | 76 | 9 | 9 |
| 16 | | 3.00 | 88 | 11 | 9 |
| 17 | | 5.00 | 88 | 12 | 7 |
| 18 | $CDCl_3$[c] | 1.00 | 26 | 3 | 7 |
| 19 | [D6]DMSO | 1.00 | 6 | 32 | 48 |
| 20[i] | | | 6 | 32 | – |
| 21[b] | | | 7 | 32 | 51 |

[a] Yields were determined by $^1$H NMR analysis. [b] Air was used. [c] 10 vol% [D6]DMSO. [d] Mixing. [e] 1 eq $NEt_3$. [f] 1 eq of $tBuNH_2$. [g] 0.1 eq of DBU. [h] 1 eq of **1e**. [i] 15 min.

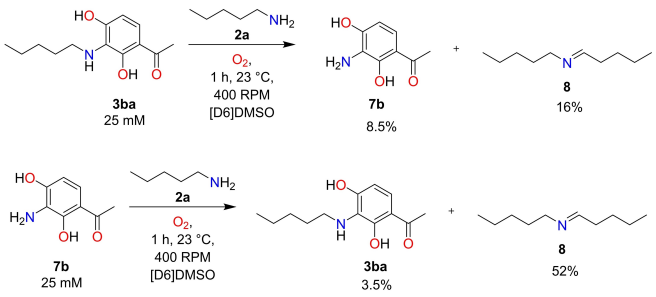


**Scheme 5.** Comparison of the oxidative deamination ability of **3ba** and **7b**.

of aminophenol **7b** with pentylamine forms only 3.5% of **3ba** and 52% of imine **8**, which is 3.5 times higher than in the example with **3ba**, indicating that transamination for aminophenol **7b** is a highly favourable process under these conditions. This observation is in line with earlier observations that aminophenols such as **7b** can inhibit fibril formation and remodel existing ones.[9d]

A distinctive feature of **1b** is the presence of an electrophilic carbonyl group, whose condensation reaction with pentylamine (**2a**) describes an extension of the overall reaction network shown as yellow area **C** in Scheme 3. Actual reactions in the area include the formation of imine **3ba**′ (from reactant phenol **1b** and **2a**) and its subsequent oxidative C–N coupling step to imine **3ba**″. The latter compound is also accessible from **3ba** through condensation with pentylamine. The overall reaction network is completed by overoxidation product **9ba** in grey area **D**, whose formation from either C–N coupling product **3ba** or from transient iminoquinone **9ba** can be detected in mass spectrometric measurements.

## Variations of the N-nucleophile

Aside from pentylamine (**2a**), several amides have been tested as side chain models for *N*-terminal lysine residues. As shown in Scheme 6, this includes a series of amino-substituted amides with increasingly large distances between these two functional groups.

The smallest of these nucleophiles are *N*-methyl glycine (**2b**) and *N*-methyl alanine (**2c**), both of which show no detectable formation of C–N coupling products with baicalein even in the presence of external bases such as DIPEA or DBU. In the homologous series of *N*-methylamido-1-aminocarboxylic amides **2d–g**, we observe a gradual increase in the yield of C6-adducts **3ad–g**, which correlates with the p$K_a$ values of these *N*-nucleophiles, reaching its maximum in the case of lysine derivatives. The similarity of the results obtained for **2a** (80%) and lysine derivative **2g**′ (78%) confirms the suitability of the former compound as a functional side chain mimic.

The regiochemistry of these coupling reactions was determined using HMBC NMR measurements, and could be confirmed independently for product **3ad** with sc-XRD of a crystal grown from heptane/EtOAc/EtOH solution (Figure 2). DFT calculations (SMD(water)/B3LYP-D3/6-31+G(d,p)) indicate this

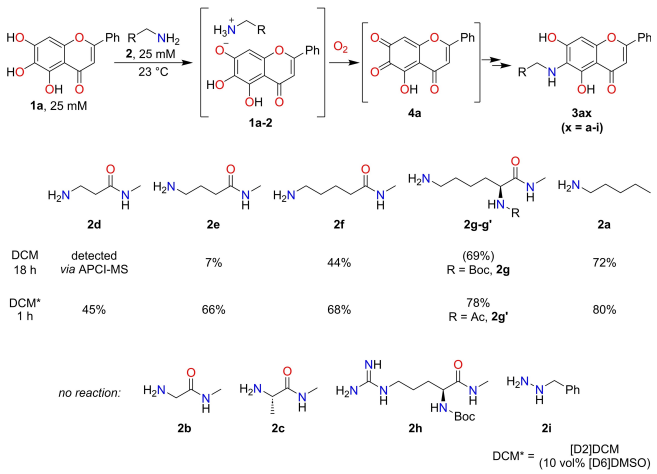


**Scheme 6.** Oxidative coupling of **1a** with various *N*-nucleophiles **2a–i**.

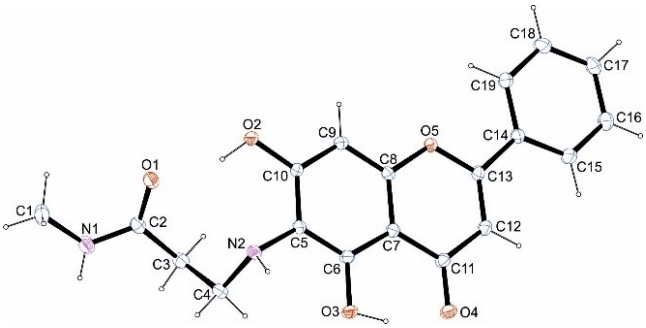


**Figure 2.** Crystal structure of coupling product **3ad** (ellipsoids shown at 25% probability level).

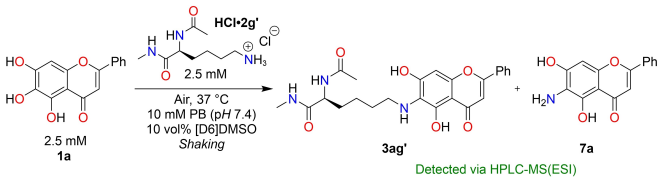


**Scheme 7.** Oxidative coupling of **1a** with *N*-Ac-Lys-NMe **2g**′ in water at pH 7.4.

regioisomer as the most thermodynamically favored (see section SI–B 6).

The applicability of the oxidative coupling reaction was also tested for arginine derivative **2h** as an alternative amino acid with basic side chain functionality and for benzyl hydrazine **2i**. Both compounds were found to yield no C–N coupling product.

The reaction of flavonoids with lysine derivatives under aqueous conditions at controlled p*H* values is directly relevant for the adduct formation of **1a** with hIAPP.[7] Based on the results obtained for other amyloidogenic peptides[9a,13] the covalent interaction is assumed to occur between the ε-$NH_2$ group of lysine and the central ring of **1a**. In order to support this mechanism in experiments with low-molecular weight models, *N*-Ac-Lys-NMe (**2g**′) was selected as a model for the *N*-terminal lysine residue in hIAPP and incubated with **1a** (2.5 mM) in 10 mM phosphate buffer (pH 7.4) at 37 °C. HPLC-MS(ESI) analysis of the reaction mixture shows the formation of covalent adduct **3ag**′ as well as the formation of the product of its hydrolysis **7a** (Scheme 7).

## Variations of the polyol electrophile

To identify factors relevant for the observed polyphenol-amine coupling process, a set of different polyphenols with structural modifications are tested. 1 eq of **2a** is mixed with the polyphenols **1a**–**p** shown in Scheme 8 in an atmosphere of pure oxygen and the product yield is determined after 1 hour of reaction time at 23 °C as a measure of the reactivity of the corresponding electrophile. In order to discuss the substituent effects observed in this benchmark reaction, we use the same (baicalein-derived) numbering scheme for all systems. Polyphenols containing an *ortho*-dihydroxyphenyl (or *ortho*-catechol)

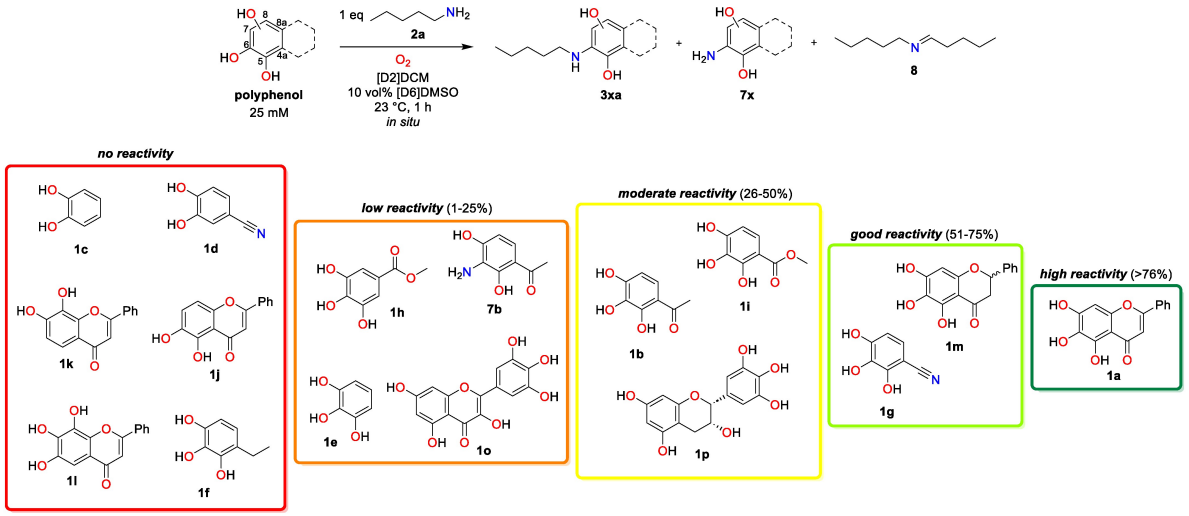


| Yield, %[a] | 1a | 1b | 1e | 1g | 1h | 1i | 1m | 1o | 1p | 7b[b] |
|---|---|---|---|---|---|---|---|---|---|---|
| **3xa** | 80% | 42% | 13% | 68% | 1.2% | 49% | 66% | 3% | 45% | 15% |
| **7x** | - | 7% | - | 4% | ND | 8% | - | ND | - | - |
| **8** | 5% | 13% | 5% | 8% | ND | 17% | 7% | ND | 4% | 7% |

**Scheme 8.** Reaction of amine **2a** with polyphenols **1a**–**o** and their propensity for forming covalent adducts. [a] Yields were determined by $^1$H NMR analysis. [b] In 24 h.

moiety exhibit no measurable reactivity towards amine **2a**. For the oxidative coupling to occur, the presence of a 1,2,3-trihydroxyphenyl (or pyrogallol) subunit appears to be required. Pyrogallol (**1e**) as the parent system of this group shows only low activity under the given conditions (13% yield of **3ea**), but reaction turnover increases significantly on introduction of an electron-withdrawing group (EWG) to the C4a-position of the pyrogallol ring. For example, a COOMe-group at C4a-position (**1i**) increases the yield of a covalent adduct **3ia** to 49%, while the same group placed at C8a-position (**1h**) significantly decreases the reactivity, giving only 1.2% of covalent adduct **3ha** under the same conditions. Increasing the electron-withdrawing ability as in cyano-substituted compound **1g** leads to even higher reaction rates and yields 68% of adduct **3ga**. The reactivity of the pyrogallol ring can be moderately enhanced through combination of an EWG at C4a and an electron donating group (EDG) at C8a as is, for example, the case in **1m** (66% yield vs 42% for **1b**) and, of course, in baicalein (**1a**). In summary, it appears that the combination of the effects of a C4a-EWG and an C8a-EDG in a pyrogallol substructure leads to the most effective formation of the C6-coupling products. To verify the proposed hypothesis, the same reaction is performed with *pseudo*-baicalein (**1l**), an isomer of the highly reactive **1a** with reversed positions of the EWG and EDG groups. Interestingly, the experiment shows no covalent adduct formation, even in the presence of 2 eq of amine **2a**.

## Quantitative Measures of Antioxidant Reactivity

The substituent effects discussed above already suggest that reaction products such as **3aa** may be better antioxidants than the respective starting polyphenol (**1a**). As a quantitative expression of the antioxidative potential of phenols **1**, **3** and **7**, we have computed the respective homolytic O–H and, where applicable, N–H bond energies (BDEs, Figure 3). These have been determined through gas phase calculations relative to that for phenol (PhOH), whose BDE(O–H) value equates to +365.0 kJ/mol.[14]

Figure 3 shows the BDE values, which directly relate to the hydrogen atom transfer (HAT) mechanism of antioxidants (see further details in SI). The lowest BDE value in each compound is marked in green characters. Comparatively small BDE(O–H) values are found for pyrogallol (**1e**), its ethyl derivative **1f** and the well-known antioxidant molecules **1o**, **1p** and **1q**.[15] All of these compounds feature a pyrogallol subunit, and irrespective of any other substituents, it is always the central of the three hydroxy groups that shows the lowest BDE value. Baicalein (**1a**) shows, somewhat surprisingly, a comparatively high BDE(O–H) value of +337 kJ/mol. This value is 30 kJ/mol higher than in pyrogallol itself and already implies, that the BDE(O–H) values alone are not sufficient to rationalize the high coupling yields observed for **1a**. Replacing the C6 hydroxyl group by amine nucleophiles leads to a reduction of the BDE(O–H) values in full agreement with stronger electron donating effects through amino *vs.* hydroxyl substituents. All compounds combining a pyrogallol subunit with an EWG at the C4a-position are located

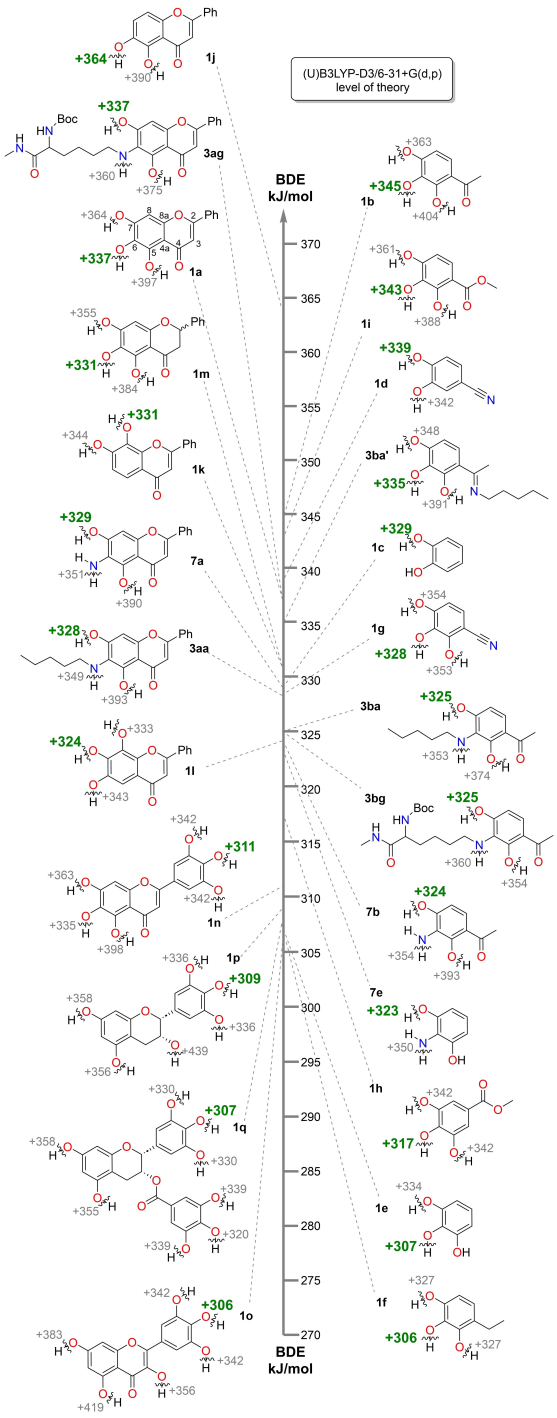


**Figure 3.** Bond dissociation enthalpy (BDE) values of selected polyphenols.

at the top of Figure 3 (with comparatively high BDE(O–H) values). Disrupting the H-bonding interaction between the EWG and the hydroxyl group at C5 (as, for example, in *pseudo*-baicalein (**1l**)) leads to a moderate reduction of BDE(O–H). Even though the BDE (O–H) values are often used to assess the antioxidant properties of polyphenols, in most cases they are not sufficient to map all aspects of antioxidative activity. Hence, the ionization potential (IP), the proton affinity (PA), and the electron transfer enthalpy (ETE) are determined at the same

level of theory in order to account for alternative mechanisms of antioxidative activity such as single-electron transfer followed by proton transfer (SET-PT), or sequential proton loss followed by electron transfer (SPLET) (see SI for details).

### Experimental Assessment of Antioxidative Activity

The antioxidant activity of the 25 compounds shown in Figure 3 was evaluated by FRAP and ORAC assays. FRAP results are presented in Figure 4a, and ORAC results in Figure 4b.

Based on both experimental assays, the studied polyphenols have higher antioxidant activity than Trolox chosen as a water-soluble reference compound. The observed FRAP values are highest for **1l** (3.40), **1n** (3.06), and **1q** (3.05), and lowest for the phenol **3ba**′ (1.26) and **7a** (1.24). The loss in antioxidative capacity observed for the aminated compounds may be related to the sensitive ionization state of the amino groups at pH 3.5 used in FRAP assays. Among the tested polyphenols the highest ORAC values are observed for **1d** (4.87), **1o** (4.40) and **1c** (3.96). FRAP and ORAC values of the compounds tested here correlate poorly (r = 0.02, See SI), an observation that has already been made in earlier studies.[16] Still, both assays show very good antioxidant abilities for the established antioxidants **1o**, **1p**, and **1q**,[15,17] as well as quite good and comparable results for baicalein (**1a**) and its derivative **1m**. Single descriptor correlations of the measured FRAP and ORAC data with the computed values described before have been analyzed with the goal of identifying possible modes of action. The FRAP data show only moderate correlations with BDE values (r = −0.52) and with PA values (r = −0.51), but the compounds with lowest BDE(O–H) values (such as **1q**, **1n**, and **1o**) are also those with lowest PA values. This is compatible with both HAT and SPLET as the limiting mechanisms in the FRAP assay measurements. The aminated compounds **3ag**, **7a**, **3ba**, **3aa** and **3bg** are those with the smallest calculated ionization potentials (IP), suggesting SET-PT as the preferred radical scavenging mechanism for these systems. The overall moderate correlations found here between the FRAP data and single descriptors may reflect the broad structural variations of the compounds considered as well as possible diverse antioxidant mechanisms. The set of 25 phenolic molecules has therefore been subdivided into the classes shown in Figure 5 in order to aid further analysis. The group of highest interest in this work is that of the pyrogallol-containing flavonoids, which shows the highest correlations between the PA and FRAP data (r = −0.88, Figure 6), and also those between the BDE and ORAC (r = −0.72, see SI). These results are best understood as the parallel existence of multiple mechanisms for antioxidative activity, which is in agreement with previous studies and irrespective of HAT often being assumed as the dominant radical-scavenging mechanism of flavonoids,[11a] the SET and SPLET mechanisms are also suggested for flavonoids such as luteolin, EGCG and curcumin.[11a,18] The mechanistic differences can then be attributed to: *i)* slight structural differences on flavonoids such as amination, intramolecular bonds and number of conjugated systems; *ii)* possible differences in the prevalence of ionization forms of some compounds;[19] and *iii)* the tendency of some polyphenols such

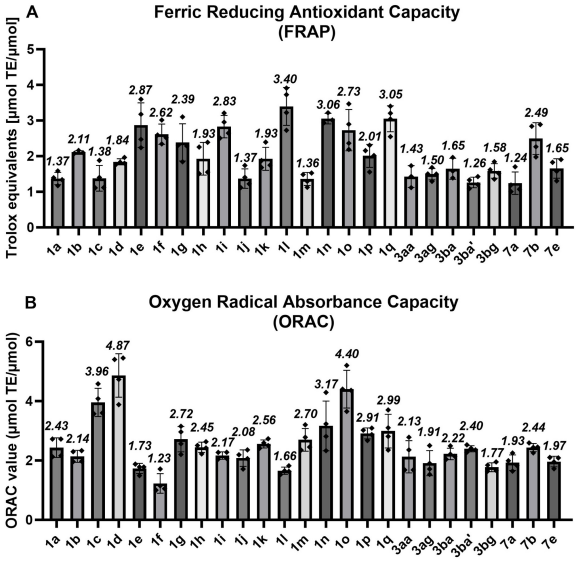


**Figure 4.** Antioxidative effects of the compounds shown in Figure 3 assessed by A) FRAP and B) ORAC.

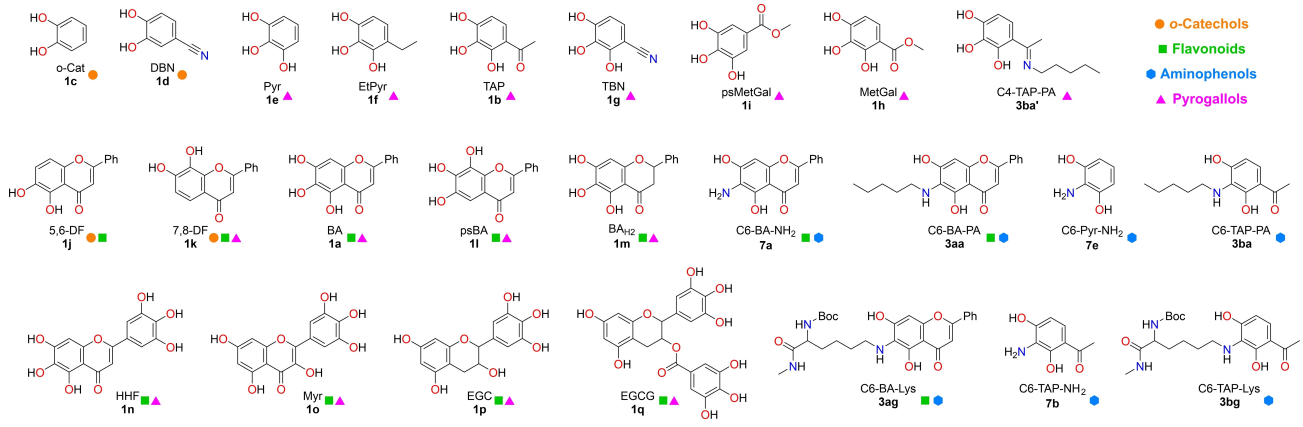


**Figure 5.** Categorization of the set of 25 compounds by four classes: *o*-catechols, pyrogallols, flavonoids and aminophenols.

as **1h**, **1o**, and **1q** to act as antioxidants and pro-oxidants under some conditions (*e.g.* high concentrations and p*H*).[20]

### Quantitative Model for Polyphenol-Amine Coupling

The chemical yields of C6-coupling product **3xa** and of imine dimer **8** directly relate to the inhibition of fibrillation of amyloidogenic peptides through the polyphenols studied here. Mapping the yields of these two compounds with a multiparametric model was therefore attempted using the experimentally measured FRAP and ORAC data, the reaction energies described above, and a larger selection of additional computational data. For a subset of 11 polyphenols, this also includes analyzing the reaction energies for selected parts of the reaction network shown in Scheme 3. This includes the Gibbs free energy for the reaction of polyphenols with pentylamine (**2a**) to yield the C6-aminated product and water described as "Pathway A" in Table 2. All of these reaction energies are negative, but actual correlation with reaction yields is low ($r = +0.15$).

Better correlations exist for other parts of the reaction network such as formation of **9xa** through disproportionation of **5xa** ($r = +0.58$) or the mostly endergonic reaction of intermediate **6xa** with either water ($r = +0.34$) or with pentylamine ($r = +0.35$). A multivariate analysis using 84 descriptors including all those described above was then performed. Descriptors from various categories are considered: class I – thermochemical properties (*e.g.* computed BDE and p$K_a$ values); class II – topology data (*e.g.* number of conjugated bonds); class III – electron distribution data such as natural bond orbital (NBO) charges; and class IV – experimental data (*e.g.* spectroscopic $^{13}$C NMR chemical shifts). Two different models were considered: 1) to predict the yields of polyphenol-amine coupling products **3xa**; and 2) to predict the yields of polyphenol-amine coupling products **3xa** together with **8**. The correlation coefficients obtained for both models are very good ($r^2 = 0.84$ and $r^2 = 0.86$, respectively). For the latter model we find best results ($r^2 = 0.86$) for a two-parameter equation combining the NBO charges at C6 in **1x**$^-$ with those at C8 in **6xa** as schematically shown in Figure 7. The inclusion of **8** as reaction product is biologically more relevant since it also accounts for the beneficial effect of polyphenols as oxidative modifiers of proteins that mediate protein polymerization by lysine-derived crosslinks.[21]

To maximize the number of compounds on the correlation, three polyphenols with no turnover are included, which could rather interfere in the equations of the model. Because of that, the experimental reaction with myricetin (**1o**) is used as positive control to validate the predictive ability of eq. 1.

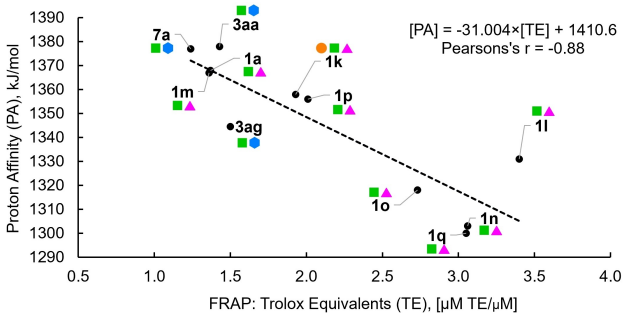


**Figure 6.** Correlation between the FRAP results (in Trolox equivalents) obtained for 11 pyrogallol-containing flavonoids from Figure 5 and their proton affinity (PA) values.

**Table 2.** Gibbs free energies ($\Delta G_{298}$, in kJ/mol) for the *o*-quinone chain A, overoxidation D and imine formation B reactions shown in Scheme 3.

| polyphenol **1x** | Pathway **A** **1x** + **2a** → **3xa** + $H_2O$ $\Delta G_{298}$, kJ/mol[a] | Pathway **D** 2×**5xa** → **3xa** + **9xa** | Pathway **B** (hydrolysis) **6xa** + $H_2O$ → **7a** + $C_5H_{10}O$ | Pathway **B** (aminolysis) **6xa** + **2a** → **7x** + **8** |
|---|---|---|---|---|
| **1a** (BA) | −33.4 | −70.4 | +1.1 | +12.1 |
| **1b** (TAP) | −31.8 | −96.0 | +2.6 | +13.5 |
| **1g** (TBN) | −30.2 | −57.8 | +1.5 | +12.4 |
| **1c** (*o*-Cat) | −34.2 | −82.3 | +5.8 | +16.7 |
| **1d** (DBN) | −40.7 | −121.2 | +2.8 | +13.7 |
| **1e** (Pyr) | −30.0 | −64.7 | +1.6 | +12.5 |
| **1h** (MetGal) | −25.0 | −89.7 | −9.8 | +1.2 |
| **1i** (psMetGal) | −26.0 | −75.2 | −1.0 | +9.9 |
| **1l** (psBA) | −33.3 | −81.5 | −4.1 | +6.8 |
| **1m** ($BA_{H2}$) | −33.9 | −52.7 | +7.6 | +18.5 |
| **1p** (EGC) | −30.1 | −86.6 | +0.8 | +11.8 |
| r for yields of **3xa** | +0.15 | +0.58 | +0.34 | +0.35 |
| r for yields of **3xa** + **8** | +0.19 | +0.57 | +0.33 | +0.34 |

[a] Pentylamine (**2a**) was used as the amine partner for all reactions. All energies are obtained using optimized geometries at the SMD(water)/B3LYP-D3/6-31 + G(d,p) level of theory. For energies calculated at DLPNO-CCSD(T)/CBS//SMD(water)/B3LYP-D3/6-31 + G(d,p) level see SI.

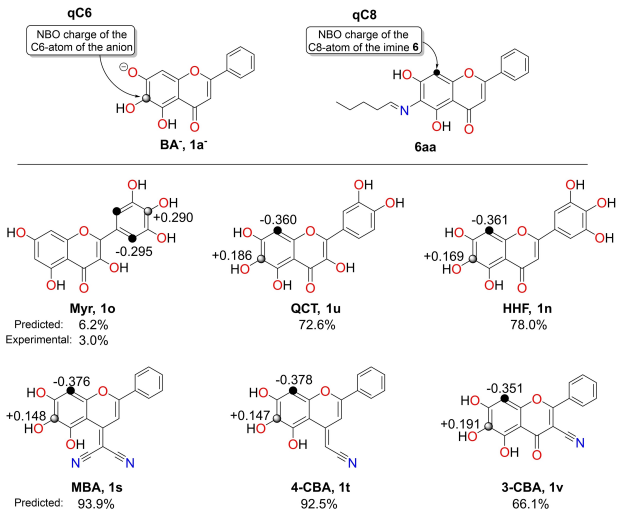


**Figure 7.** Molecular structures of the anionic form of **1a**$^-$ (**BA**$^-$), **6aa**, **1o**, **1n**, quercetagetin (**1u**), malononitrile-baicalein (**1s**), 4-cyano-baicalein (**1t**), and 3-cyano-baicalein (**1v**).

$$\begin{aligned} [3\boldsymbol{xa}+8] \\ \textit{predicted yield}, \% \\ -568.5468 \times qC8[6\boldsymbol{xa}] \end{aligned} = -79.3891 - 283.0536 \times qC6[1\boldsymbol{x}^-] \quad (1)$$

The predicted combined yield (**3oa**+**8**) is 6.2%, which agrees closely with the small amount observed experimentally (3%, see Scheme 8). Eq. 1 was therefore used to predict the C6-amination yields for a small set of yet unknown baicalein derivatives (Figure 7). From this small compound set, the results for cyano-substituted systems **1s** and **1t** appear to be most promising. Whether or not these compounds will be effective as inhibitors of fibril formation and protein aggregation will, of course, also depend on other factors such as their solubility in biologically relevant media.

## Conclusions

In this article, we report a mechanistic study into the oxidative coupling between polyphenols and amines. Large datasets of both reactants under different buffer conditions are tested. We conclude that, from a mechanistic point of view, the oxidative coupling between polyphenols and *N*-nucleophiles occurs by a multi-step process best described as an oxidative dearomatization, amination and reductive amination (ODARA). Detailed mechanistic insights are obtained using a DCM (10 vol% [D6]DMSO) reaction medium. The reaction between baicalein and lysine derivatives under aqueous conditions, however, has also been tested successfully. Hence, we conclude that the studied molecules follow the ODARA process in a physiologic environment, and they can be used for biological and medicinal purposes.

The bond dissociation enthalpy (BDE) calculations indicate that the absence of the H-bridge C5-OH···O–C4 and the C6-regioselective amination of flavonoids, using baicalein as model, improves the antioxidant ability (BDE decreases by *ca.* 9–13 kJ/mol). FRAP and ORAC results suggest that all compounds considered here show better antioxidant abilities than Trolox. The results from both *in silico* and *in vitro* antioxidant approaches allows us to conclude that myricetin, EGCG, HHF, pyrogallol and its derivatives are the compounds with highest antioxidant power in the tested dataset. Also, the correlation between the thermodynamic properties (BDE, proton affinity) and the FRAP and ORAC assays supports the absence of a dominant radical-scavenging mechanism, but rather points to a multitude of pathways (SET, SPLET and HAT) being active in parallel.

Multivariate analysis employing a larger set of focused descriptors allowed development of two-component models for the prediction of chemical reaction yields. The models use atomic charges of transient intermediates of the ODARA process as descriptors. Using these models, we predict new baicalein derivatives as crosslinking agents for amyloidogenic peptides.

## Supporting Information

The authors have cited additional references within the Supporting Information.[23–87]

## Acknowledgements

NFB acknowledges the support from the scientific employment stimulus – individual call of 2018 (CEECIND/02017/2018). Open Access funding enabled and organized by Projekt DEAL.

## Conflict of Interests

The authors declare no conflict of interest.

## Data Availability Statement

The data that support the findings of this study are available in the supplementary material of this article.

**Keywords:** Cross-coupling · DFT · Flavonoids · Oxidation · Predictive Model

[1] a) C. Anthony, M. Ghosh, C. C. Blake, *Biochem. J.* **1994**, *304*, 665–674; b) C. Anthony, *Biochem. J.* **1996**, *320*, 697–711; c) A. Lang, J. P. Klinman, in *eLS*, John Wiley & Sons, **2013**.
[2] a) M. Largeron, M.-B. Fleury, *Angew. Chem. Int. Ed.* **2012**, *51*, 5409–5412; b) H. Yuan, W.-J. Yoo, H. Miyamura, S. Kobayashi, *J. Am. Chem. Soc.* **2012**, *134*, 13970–13973; c) A. E. Wendlandt, S. S. Stahl, *J. Am. Chem. Soc.* **2014**, *136*, 506–512; d) R. Zhang, Y. Qin, L. Zhang, S. Luo, *Org. Lett.* **2017**, *19*, 5629–5632; e) J. Baek, T. Si, H. Y. Kim, K. Oh, *Org. Lett.* **2022**, *24*, 4982–4986.
[3] a) K. Kida, M. Suzuki, A. Takagaki, F. Nanjo, *Biosci. Biotechnol. Biochem.* **2002**, *66*, 373–377; b) K. Hashida, R. Makino, S. Ohara, *Holzforschung* **2009**, *63*, 319–326.

[4] F. Braghiroli, V. Fierro, A. Pizzi, K. Rode, W. Radke, L. Delmotte, J. Parmentier, A. Celzard, *Ind. Crops Prod.* **2013**, *44*, 330–335.
[5] a) M. Largeron, A. Neudorffer, M.-B. Fleury, *Tetrahedron Lett.* **1998**, *39*, 5035–5038; b) R. Larget, B. Lockhart, B. Pfeiffer, A. Neudorffer, M.-B. Fleury, M. Largeron, *Bioorg. Med. Chem. Lett.* **1999**, *9*, 2929–2934; c) M. Largeron, M.-B. Fleury, *J. Org. Chem.* **2000**, *65*, 8874–8881; d) R. Larget, B. Lockhart, P. Renard, M. Largeron, *Bioorg. Med. Chem. Lett.* **2000**, *10*, 835–838.
[6] a) S. Zhang, R. Wang, Y. Zhao, F. S. Tareq, S. Sang, *Mol. Nutr. Food Res.* **2019**, *63*, 1900203; b) S. Zhang, Y. Zhao, C. Ohland, C. Jobin, S. Sang, *Free Radical Biol. Med.* **2019**, *131*, 332–344; c) S. Zhang, R. Wang, Y. Zhao, F. S. Tareq, S. Sang, *Chem. Res. Toxicol.* **2020**, *33*, 2181–2188.
[7] P. Velander, L. Wu, W. K. Ray, R. F. Helm, B. Xu, *Biochemistry* **2016**, *55*, 4255–4258.
[8] N. F. Brás, S. S. Ashirbaev, H. Zipse, *Chem. Eur. J.* **2022**, *28*, e202104240.
[9] a) M. Zhu, S. Rajamani, J. Kaylor, S. Han, F. Zhou, A. L. Fink, *J. Biol. Chem.* **2004**, *279*, 26846–26857; b) F. L. Palhano, J. Lee, N. P. Grimster, J. W. Kelly, *J. Am. Chem. Soc.* **2013**, *135*, 7503–7510; c) M. Furuhashi, Y. Hatasa, S. Kawamura, T. Shibata, M. Akagawa, K. Uchida, *Biochemistry* **2017**, *56*, 4701–4712; d) L. Fernandes, N. Moraes, F. S. Sagrillo, A. V. Magalhães, M. C. de Moraes, L. Romão, J. W. Kelly, D. Foguel, N. P. Grimster, F. L. Palhano, *ACS Chem. Neurosci.* **2017**, *8*, 1704–1712; e) P. Velander, L. Wu, S. B. Hildreth, N. J. Vogelaar, B. Mukhopadhyay, R. F. Helm, S. Zhang, B. Xu, *Pharmacol. Res.* **2022**, *184*, 106409.
[10] X. Liu, Q. Song, X. Li, Y. Chen, C. Liu, X. Zhu, J. Liu, D. Granato, Y. Wang, J. Huang, *Food Chem.* **2021**, *361*, 130071.
[11] a) J. S. Wright, E. R. Johnson, G. A. DiLabio, *J. Am. Chem. Soc.* **2001**, *123*, 1173–1183; b) H. F. Ji, H. Y. Zhang, *New J. Chem.* **2005**, *29*, 535–537; c) A. Y. Akyeva, A. V. Kansuzyan, K. S. Vukich, L. Kuhn, E. A. Saverina, M. E. Minyaev, V. M. Pechennikov, M. P. Egorov, I. V. Alabugin, S. V. Vorobyev, M. A. Syroeshkin, *J. Org. Chem.* **2022**, *87*, 5371–5384.
[12] C. L. Perrin, J. B. Nielson, *Annu. Rev. Phys. Chem.* **1997**, *48*, 511–544.
[13] S.-m. Song, Y.-x. Wang, L.-m. Xiong, L.-b. Qu, M.-t. Xu, *Chem. Res. Chin. Univ.* **2013**, *29*, 20–25.
[14] J. Hioe, H. Zipse, *Faraday Discuss.* **2010**, *145*, 301–313 and subsequent discussion, p. 381–409.
[15] a) K. Aaby, E. Hvattum, G. Skrede, *J. Agric. Food Chem.* **2004**, *52*, 4595–4603; b) D. Zhang, Y. Liu, L. Chu, Y. Wei, D. Wang, S. Cai, F. Zhou, B. Ji, *J. Phys. Chem. A* **2013**, *117*, 1784–1794.
[16] a) S. Dudonne, X. Vitrac, P. Coutiere, M. Woillez, J. M. Merillon, *J. Agric. Food Chem.* **2009**, *57*, 1768–1774; b) L. Lespade, S. Bercion, *Free Radical Res.* **2012**, *46*, 346–358.
[17] D. Huang, B. Ou, M. Hampsch-Woodill, J. A. Flanagan, R. L. Prior, *J. Agric. Food Chem.* **2002**, *50*, 4437–4444.
[18] a) S. V. Jovanovic, Y. Hara, S. Steenken, M. G. Simic, *J. Am. Chem. Soc.* **1995**, *117*, 9881–9888; b) G. Litwinienko, K. U. Ingold, *J. Org. Chem.* **2005**, *70*, 8982–8990.
[19] M. Musialik, R. Kuzmicz, T. S. Pawlowski, G. Litwinienko, *J. Org. Chem.* **2009**, *74*, 2699–2709.
[20] a) G. Cao, E. Sofic, R. L. Prior, *Free Radical Biol. Med.* **1997**, *22*, 749–760; b) Q. V. Vo, P. C. Nam, N. M. Thong, N. T. Trung, C. D. Phan, A. Mechler, *ACS Omega* **2019**, *4*, 8935–8942.
[21] a) K. Yamaguchi, M. Itakura, R. Kitazawa, S.-Y. Lim, K. Nagata, T. Shibata, M. Akagawa, K. Uchida, *J. Biol. Chem.* **2021**, *297*; b) K. Yamaguchi, M. Itakura, M. Tsukamoto, S. Y. Lim, K. Uchida, *J. Biol. Chem.* **2022**, *298*, 102529.
[22] Deposition numbers 2296456 (for **1a**), 2296457 (for **1b**), 2296458 (for **3aa**), 2296459 (for **3ba**), 2296460 (for **7b**), 2296461 (for **3ga**), 2296462 (for **3ia**), and 2296463 (for **3ad**) contain the supplementary crystallographic data for this paper. These data are provided free of charge by the joint Cambridge Crystallographic Data Centre and Fachinformationszentrum Karlsruhe Access Structures service.
[23] G. Milordini, E. Zacco, M. Percival, R. Puglisi, F. Dal Piaz, P. Temussi, A. Pastore, *Front. Mol. Biosci.* **2020**, *7*, 1–13.
[24] I.-H. Um, E. Y. Kim, H.-R. Park, S.-E. Jeon, *J. Org. Chem.* **2006**, *71*, 2302–2306.
[25] H. K. Hall Jr., *J. Am. Chem. Soc.* **1957**, *79*, 5441–5444.
[26] R. B. Martin, A. Parcell, R. I. Hedrick, *J. Am. Chem. Soc.* **1964**, *86*, 2406–2413.
[27] Z. Feng, J. Zhou, X. Shang, G. Kuang, J. Han, L. Lu, L. Zhang, *Pharm. Biol.* **2017**, *55*, 1177–1184.
[28] J. M. Herrero-Martínez, M. Sanmartin, M. Rosés, E. Bosch, C. Ràfols, *Electrophoresis* **2005**, *26*, 1886–1895.
[29] a) I. Miroshnyk, S. Mirza, N. Sandler, *Expert Opin. Drug Delivery* **2009**, *6*, 333–341; b) G. Bolla, A. Nangia, *Chem. Commun.* **2016**, *52*, 8342–8360.
[30] S. Chattoraj, L. Shi, C. C. Sun, *CrystEngComm* **2010**, *12*, 2466–2472.
[31] C. C. Sun, H. Hou, *Cryst. Growth Des.* **2008**, *8*, 1575–1579.
[32] S. Saito, J. Kawabata, *Tetrahedron* **2005**, *61*, 8101–8108.
[33] J. Bomon, E. Van Den Broeck, M. Bal, Y. Liao, S. Sergeyev, V. Van Speybroeck, B. F. Sels, B. U. W. Maes, *Angew. Chem. Int. Ed.* **2020**, *59*, 3063–3068.
[34] G. Baisch, B. Wagner, R. Öhrlein, *Tetrahedron* **2010**, *66*, 3742–3748.
[35] M. K. Srinatha, S. Poppe, G. Shanker, M. Alaasar, C. Tschierske, *J. Mol. Liq.* **2020**, *317*, 114244.
[36] J. K. Augustine, A. Bombrun, R. N. Atta, *Synlett* **2011**, *2011*, 2223–2227.
[37] G. Degotte, H. Pendeville, C. Di Chio, R. Ettari, B. Pirotte, M. Frédérich, P. Francotte, *RSC Med. Chem.* **2023**, *14*, 715–733.
[38] X. Qin, L. Yang, P. Liu, L. Yang, L. Chen, L. Hu, M. Jiang, *Bioorg. Chem.* **2021**, *110*, 104743.
[39] a) C. Li, T. Chen, B. Li, G. Xiao, W. Tang, *Angew. Chem. Int. Ed.* **2015**, *54*, 3792–3796; b) M. Matsumoto, K. Kobayashi, Y. Hotta, *J. Org. Chem.* **1984**, *49*, 4740–4741.
[40] K. Ishikawa, K. Takahashi, S. Hosoi, H. Takeda, H. Yoshida, D. Wakana, M. Tsubuki, F. Sato, M. Tojo, T. Hosoe, *J. Antibiot.* **2019**, *72*, 71–78.
[41] M. Satyanarayana, P. Tiwari, B. K. Tripathi, A. K. Srivastava, R. Pratap, *Bioorg. Med. Chem.* **2004**, *12*, 883–889.
[42] Y. Huang, G. Sun, P. Wang, R. Shi, Y. Zhang, X. Wen, H. Sun, C. Chen, *Bioorg. Med. Chem. Lett.* **2018**, *28*, 2957–2960.
[43] B. B. Park, J. W. Choi, D. Park, D. Choi, J. Paek, H. J. Kim, S.-Y. Son, A. U. Mushtaq, H. Shin, S. H. Kim, Y. Zhou, T. Lim, J. Y. Park, J.-Y. Baek, K. Kim, H. Kwon, S.-H. Son, K. Y. Chung, H.-J. Jeong, H.-M. Kim, Y. W. Jung, K. Lee, K. Y. Lee, Y. Byun, Y. H. Jeon, *Sci. Rep.* **2019**, *9*, 8762.
[44] H. Gao, J. Kawabata, *Bioorg. Med. Chem.* **2005**, *13*, 1661–1671.
[45] Z.-P. Xiao, Z.-Y. Peng, J.-J. Dong, J. He, H. Ouyang, Y.-T. Feng, C.-L. Lu, W.-Q. Lin, J.-X. Wang, Y.-P. Xiang, H.-L. Zhu, *Eur. J. Med. Chem.* **2013**, *63*, 685–695.
[46] M. Y. Zhang, R. A. Barrow, *Org. Lett.* **2017**, *19*, 2302–2305.
[47] L. K. Tsou, M. Lara-Tejero, J. RoseFigura, Z. J. Zhang, Y.-C. Wang, J. S. Yount, M. Lefebre, P. D. Dossa, J. Kato, F. Guan, W. Lam, Y.-C. Cheng, J. E. Galán, H. C. Hang, *J. Am. Chem. Soc.* **2016**, *138*, 2209–2218.
[48] J. Hierold, S. Baek, R. Rieger, T.-G. Lim, S. Zakpur, M. Arciniega, K. W. Lee, R. Huber, L. F. Tietze, *Chem. Eur. J.* **2015**, *21*, 16887–16894.
[49] J.-N. Yang, J.-Y. Yang, J. Cao, X.-Q. Zhou, W. Mian, Y. Hui, W.-H. Chen, *Chem. Nat. Compd.* **2020**, *56*, 539–541.
[50] H. Gao, J. Kawabata, *Biosci. Biotechnol. Biochem.* **2004**, *68*, 1858–1864.
[51] R. Long, C. Tang, J. Xu, T. Li, C. Tong, Y. Guo, S. Shi, D. Wang, *Chem. Commun.* **2019**, *55*, 10912–10915.
[52] Z.-W. Hou, C.-H. Chen, J.-P. Ke, Y.-Y. Zhang, Y. Qi, S.-Y. Liu, Z. Yang, J.-M. Ning, G.-H. Bao, *J. Agric. Food Chem.* **2022**, *70*, 136–148.
[53] T. Klingel, M. Hadamjetz, A. Fischer, D. Wefers, *Carbohydr. Res.* **2019**, *483*, 107741.
[54] R. H. Boutin, G. M. Loudon, *J. Org. Chem.* **1984**, *49*, 4277–4284.
[55] R. M. Keefer, L. J. Andrews, *J. Am. Chem. Soc.* **1962**, *84*, 941–945.
[56] T. L. Greaves, A. Weerawardena, C. Fong, I. Krodkiewska, C. J. Drummond, *J. Phys. Chem. B* **2006**, *110*, 22479–22487.
[57] T. L. Greaves, K. Ha, B. W. Muir, S. C. Howard, A. Weerawardena, N. Kirby, C. J. Drummond, *Phys. Chem. Chem. Phys.* **2015**, *17*, 2357–2365.
[58] L. Samulis, N. C. O. Tomkinson, *Tetrahedron* **2011**, *67*, 4263–4267.
[59] T. Morack, C. Mück-Lichtenfeld, R. Gilmour, *Angew. Chem. Int. Ed.* **2019**, *58*, 1208–1212.
[60] D. M. Shendage, R. Fröhlich, G. Haufe, *Org. Lett.* **2004**, *6*, 3675–3678.
[61] Pfizer, *EP1097706 (A1)*, **2001**.
[62] J. A. Davies, C. H. Hassall, I. H. Rogers, *J. Chem. Soc. C* **1969**, 1358–1363.
[63] Johnson & J Johnson, *WO2022/53010 (A1)*, **2022**.
[64] N. Sakai, M. Lista, O. Kel, S.-i. Sakurai, D. Emery, J. Mareda, E. Vauthey, S. Matile, *J. Am. Chem. Soc.* **2011**, *133*, 15224–15227.
[65] N. M. Naidenova, R. A. Arsatyants, *Chem. Nat. Compd.* **1974**, *10*, 508–511.
[66] H. Nakamura, S. Lee, S. Ono, T. Kato, H. Aoyagi, *Int. J. Pept. Protein Res.* **1990**, *36*, 471–475.
[67] G. P. Dado, S. H. Gellman, *J. Am. Chem. Soc.* **1994**, *116*, 1054–1062.
[68] A. R. Ekkati, A. A. Campanali, A. I. Abouelatta, M. Shamoun, S. Kalapugama, M. Kelley, J. J. Kodanko, *Amino Acids* **2010**, *38*, 747–751.
[69] R. F. Sweis, Z. Wang, M. Algire, C. H. Arrowsmith, P. J. Brown, G. G. Chiang, J. Guo, C. G. Jakob, S. Kennedy, F. Li, D. Maag, B. Shaw, N. B. Soni, M. Vedadi, W. N. Pappano, *ACS Med. Chem. Lett.* **2015**, *6*, 695–700.
[70] D. Xu, A. Chiaroni, M.-B. Fleury, M. Largeron, *J. Org. Chem.* **2006**, *71*, 6374–6381.
[71] R. Pasceri, D. Siegel, D. Ross, C. J. Moody, *J. Med. Chem.* **2013**, *56*, 3310–3317.
[72] A. D. Becke, *J. Chem. Phys.* **1993**, *98*, 5648–5652.

[73] S. Grimme, J. Antony, S. Ehrlich, H. Krieg, *J. Chem. Phys.* **2010**, *132*, 154104.
[74] P. C. Hariharan, J. A. Pople, *Theor. Chim. Acta* **1973**, *28*, 213–222.
[75] A. V. Marenich, C. J. Cramer, D. G. Truhlar, *J. Phys. Chem. B* **2009**, *113*, 6378–6396.
[76] T. H. Dunning, *J. Chem. Phys.* **1989**, *90*, 1007–1023.
[77] G. W. T. M. J. Frisch, H. B. Schlegel, G. E. Scuseria, M. A. Robb, J. R. Cheeseman, G. Scalmani, V. Barone, G. A. Petersson, H. Nakatsuji, X. Li, M. Caricato, A. Marenich, J. Bloino, B. G. Janesko, R. Gomperts, B. Mennucci, H. P. Hratchian, J. V. Ortiz, A. F. Izmaylov, J. L. Sonnenberg, D. Williams-Young, F. Ding, F. Lipparini, F. Egidi, J. Goings, B. Peng, A. Petrone, T. Henderson, D. Ranasinghe, V. G. Zakrzewski, J. Gao, N. Rega, G. Zheng, W. Liang, M. Hada, M. Ehara, K. Toyota, R. Fukuda, J. Hasegawa, M. Ishida, T. Nakajima, Y. Honda, O. Kitao, H. Nakai, T. Vreven, K. Throssell, J. A. Montgomery, Jr., J. E. Peralta, F. Ogliaro, M. Bearpark, J. J. Heyd, E. Brothers, K. N. Kudin, V. N. Staroverov, T. Keith, R. Kobayashi, J. Normand, K. Raghavachari, A. Rendell, J. C. Burant, S. S. Iyengar, J. Tomasi, M. Cossi, J. M. Millam, M. Klene, C. Adamo, R. Cammi, J. W. Ochterski, R. L. Martin, K. Morokuma, O. Farkas, J. B. Foresman, D. J. Fox, Gaussian, Inc., *Gaussian 09*, **2016**.
[78] F. Neese, F. Wennmohs, U. Becker, C. Riplinger, *J. Chem. Phys.* **2020**, *152*, 224108.
[79] Schrödinger Release 2019–2: Jaguar, Schrödinger, LLC, **2019**.
[80] E. Klein, V. Lukes, *J. Phys. Chem. A* **2006**, *110*, 12312–12320.
[81] I. F. F. Benzie, J. J. Strain, *Anal. Biochem.* **1996**, *239*, 70–76.
[82] J. M. Gostner, S. Schroecksnadel, M. Jenny, A. Klein, F. Ueberall, H. Schennach, D. Fuchs, *J. Am. Coll. Nutr.* **2015**, *34*, 212–223.
[83] R. L. Prior, X. Wu, K. Schaich, *J. Agric. Food Chem.* **2005**, *53*, 4290–4302.
[84] a) N. L. Haworth, Q. Wang, M. L. Coote, *J. Phys. Chem. A* **2017**, *121*, 5217–5225; b) P. G. Seybold, G. C. Shields, *Wiley Interdiscip. Rev.: Comput. Mol. Sci.* **2015**, *5*, 290–297.
[85] Y. Fu, L. Liu, R. Q. Li, R. Liu, Q. X. Guo, *J. Am. Chem. Soc.* **2004**, *126*, 814–822.
[86] A. E. Reed, R. B. Weinstock, F. Weinhold, *J. Chem. Phys.* **1985**, *83*, 735–746.
[87] V. Korotenko, H. Zipse, *J. Comp. Chem.* **2023**, *45*, 101–114.

Manuscript received: November 15, 2023
Accepted manuscript online: November 29, 2023
Version of record online: January 10, 2024